STUDY OF THE FLUX DENSITY VARIATION ALONG SATURN'S RING OBSERVED FROM NATIONAL OBSERVATORY, NAGARKOT, NEPAL

B. Aryal*, **H. K. Nupane*** and **S. R. Shahi****
*Central department of Physics, Tribhuvan University, Kirtipur, Nepal.
**B.P. Koirala Memorial Planetarium, Observatory and Science Museum Development Board, Ministry of Science and Technology, Singhadurbar, Kathmandu, Nepal.

Abstract: We present a study of relative flux density along the Saturn's ring. The image of the planet Saturn is taken from National Observatory located at Nagarkot, Nepal during January to March, 2010. Sixteen inch Schmidt-Cassegrain telescope is used to capture the image. The image is processed in the software ALADIN2.5. We have studied the flux density variation along Saturn's ring from eastern to western region. The observed two-dimensional image of the ring of the planet Saturn is divided into five regions namely far-eastern, mid-eastern, middle, mid-western, far-western. We found that the total flux sometimes increases and sometimes decreases showing peak values at different regions along the ring. However, in the middle (across the planet), we found a fairly homogeneous emission. We took data of relative flux density in each pixel in these regions. The minimum and maximum values of flux density are found to lie in the range (5.9 – 12.7) x 10^{-7} MJy/str. The absorption feature is found to be prominent in western region.

Key-words: Observation; Telescope; Saturn; Flux density.

INTRODUCTION

Saturn is the sixth planet from the Sun and the second largest planet in the Solar System, after Jupiter. The planet Saturn is composed of hydrogen, with small proportions of helium and trace elements[1]. It is surrounded by a system of rings that can be seen though a small amateur telescope. It is the only planet with rings substantial enough to be seen easily. However, this planet is unique in other ways. It is the least dense of the planets[2]. Saturn, like Jupiter, does not pass through phases; it always appears full or almost full. Its brilliance in the sky, as we see it, changes because its distance from us varies. In general, the greater the angle between Saturn and the Sun, the brighter Saturn appears as seen from Earth. The brilliance of Saturn is also affected by the angle at which the rings are presented to us. If the rings are edge-on, the planet looks dimmer at a given distance from us than if the rings are seen from above or below. Saturn takes 29 x 1/2 Earth years to make a complete revolution around the Sun with respect to the distant stars. Thus Saturn reaches an opposition approximately once every 12 x 1/2 Earth months[2]. The Saturnian rings can be seen even with a small telescope. The rings were discovered by Galileo Galilei in 1610; only 45 years later did Christian Huygens establish that the formation observed was actually a ring, and not two oddly behaving bulbs, as they appeared to Galileo. In 1857 James Clerk Maxwell showed theoretically that the rings cannot be solid but must be composed of small particles[3]. The rings are made of normal water ice. The size of the ring particles ranges from microns to truck-size chunks. Most of the particles are in range of centimetres to metres. The width of the ring system is more than 60,000 km (about the radius of Saturn) and thickness, at most 100 m, and possibly only a few metres. Cassini spacecraft discovered also molecular oxygen around the rings, probably as a product of the disintegration of water ice from the rings[3].

In the present work, we intend to study the flux density variation along Saturn's ring in the image captured by 16-inch LX200GPS Schmidt-Cassegrain Telescope located at the Nagarkot observatory during November 2008. The Schmidt-Cassegrain is a catadioptric telescope that combines a cassegrain rector's optical path with a Schmidt corrector plate to make a compact astronomical instrument that uses simple spherical surfaces[4]. This is an optical telescope. Optical astronomy refers to the observation and study of light. It includes the non-visible and visible light in the electromagnetic spectrum. In all forms of observational astronomy, we collect information about the heavenly bodies using telescopes and analyze this information to come to valuable predictions and conclusions. In optical astronomy, we take into account visible light while in other forms, we use

Author for Correspondence: B. Aryal, Central department of Physics, Tribhuvan University, Kirtipur, Nepal. E-mail: binil.aryal@uibk.ac.at

other wavelengths of the electromagnetic spectrum. Optical images are drawn by hand, with information from photographic devices and later on using digital detectors, particularly CCD (charge coupled devices).

The prime objectives of this work are as follows: (1) We intend to operate and calibrate the telescope named 1600 LX200GPS Schmidt-Cassegrain" installed in the National Observatory located at Nagarkot, Nepal. (2) We intend to carry out a few observational runs in the period 2008-2010 focusing the planets and their moons. (3) We focus our attention to the ring of the planet Saturn. Our interest is to capture Saturn's image and process them in the data reduction software. (4) Finally, we intend to discuss the cause of selective absorption in the ring of the planet Saturn.

OBSERVATION

Nagarkot is located at latitude 27°41' 06" N and longitude 85°31' 00" E, 32 km east of the capital city, Kathmandu. High altitude, clear sky, secure place, narrow population and noiseless environment are the basic features of Nagarkot that provided the idea of constructing the observatory there. Because of its high altitude, the weather is cold throughout the year. Most of the time the climatic condition is a bit humid, therefore, to minimize errors owing to humidity, we used an electric absorbent inside the dome while taking observations. The National Observatory at Nagarkot is the only observatory in our nation and is also popular as Nagarkot observatory. It constitutes a well built two-storey building in which a 1600 LX200GPS Schmidt-Cassegrain telescope has been installed (Fig. 1).

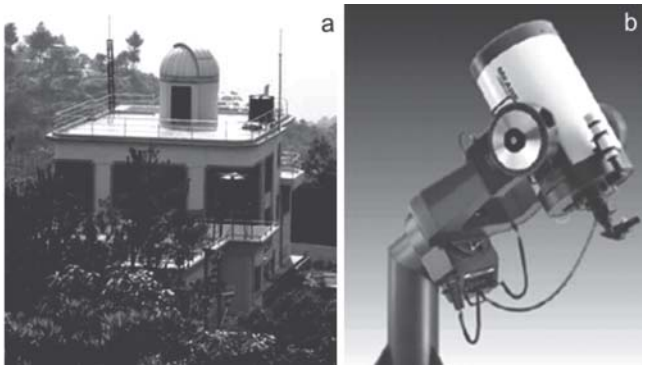

Figure 1: (a) A scenic view of National Observatory at Nagarkot. (b) Meade 1600 LX200GPS Schmidt-Cassegrain telescope.

We took observation in four sessions. The very first session was in November, 2009. It was winter, the sky was clear but bit humid. We tried to take observations under slightly humid conditions. Since it was our first visit, we spent the entire night trying to learn the techniques to handle the telescope and to produce images. Unfortunately, the images that we obtained were not satisfactory; they were absurd. The second time that we went there was in March, 2010. The winter was on its brink but the sky was not clear the entire night. However, we tried to take images whenever possible. By that time we had learned to handle the telescope properly. The image of the planet Jupiter that we worked on belongs to this session. The major achievement that we made was in the third session, during October, 2009. We were able to produce focused images. However, we had one more session in January, 2010. In that session, we produced images of not only Jupiter, but also of Saturn, moon (of Earth) and the star Polaris (Fig. 2).

We used the software CYBERSKY3.0 in order to know the objects in the sky[4]. It is an accurate planetarium program that provides an excellent way to learn about astronomy and explore the sky visible in the distant past, the present, and the future. The program makes it easy to identify the objects we see in the sky and find the objects we want to see. Before observing any object, we must define a reference frame with the telescope at its center. For this we took into account two prominent stars - Rigel and Betelgeuse. In the select menu of the telescope, we chose the two-star alignment. We manually set the telescope so that the Rigel was at the center of the field of view. After this star was set in the memory of the telescope, we set it again to focus on the Betelgeuse. When this star was set in the memory, we got the message "Alignment Successful". This message ensured that the reference frame was set and we were ready to use the telescope to view any possible object in the sky. Once a reference frame is set, the telescope works automatically as per the commands given to it through the AUTOSTAR II handbox. For example, when we give the command to go to the planet Saturn, the telescope would rotate itself to focus on the Saturn. The planet would appear in or near the field of view, depending on the accuracy with which we fix a reference frame. Once the telescope aligns itself to focus on the desired object, the only effort we have to make is to bring it in the

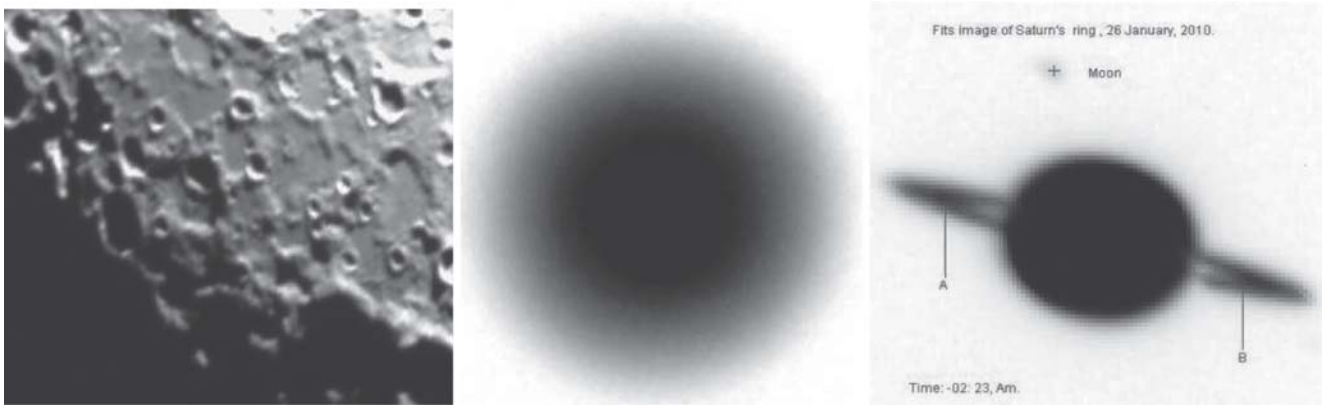

Figure 2: FITS images of moon's surface (left) Jupiter (middle) and Saturn (right) taken from National Observatory, Nagarkot during January 2010.

center of the field of view. Once the desired object appears in the center of field of view of the telescope, the eyepiece is replaced by a webcam connected to the computer. The software that we used to obtain the images on the computer is AUTOSTAR SUITE3.08[5].

There are two simultaneous processes that should be followed to remove the unwanted noise from the image obtained. The first one is to obtain a dark frame and subtract it from the raw light image. The other one is to obtain a at field image and use it to correct for variations in pixel response uniformity across the area of our dark-subtracted image.

IMAGE PROCESSING

Telescope collects the photons emitted from real three-dimensional object in a two-dimensional projection. However, to proceed further with the image, we need to locate its center or suitable reference position. There is an option in the image-processing part of AUTOSTAR SUITE that enables us to locate the center approximately. The further processing of the FITS image was done in ALADIN2.5. ALADIN, an interactive sky atlas developed at Centre de Donnees astronomiques de Strasbourg (CDS) in France, is a service providing simultaneous access to digitized images of the sky, astronomical catalogues, and databases. The driving motivation is to facilitate direct, visual comparison of observational data at any wavelength with images of the optical sky, and with reference catalogues. On our FITS image, we created contours of iso-potential (in our case relative flux density) surfaces.

RESULTS

In this section we give the results concerning the variation of relative flux density in and around the planet Jupiter. For this we used the image captured by us using Meade 16-inch LX200GPS Schmidt-Cassegrain telescope at Nagarkot Observatory during March, 2009. The values of the relative flux density for these lines have been obtained from ALADIN2.5 while the associated graphs have been derived from ORIGIN5.0.

We classified the ring into 5 regions namely, far-eastern (region 1i), mid-eastern (region 2i), eastern (region 3i), middle region (region 4), western (region 3ii), mid-western (region 2ii) and far-western (region 1ii) (see left panel of Fig. 3). The variation of relative flux density along far-eastern to far-western is shown in Fig. 3 (right). In this figure a homogeneous pattern can be seen in the left and right side (region 1i & 1ii; region 2i & 2ii and region 3i & 3ii. In the middle a steady and maximum value of relative flux density is seen (region 4). The first region (region-1i) represents the region from the far eastern to the maxima of the eastern contour. This is the region where the inclination of ring is maximum. Similarly, the last region (region-1ii) represents the far western to the maxima of the western contour, as shown in Fig. 3. The values of the relative flux density from far-eastern to the far-western region are listed in Table 1.

At first we study and compare the relative flux densities of the regions 1i & 1ii (Fig. 4). In order to study the variation of relative flux density, we have plotted the graph between pixel number and relative flux density, shown in Fig. 4. In the region-1i, the values of relative flux density are found to increase from 24.55 to 122.88. It should be remembered that the value of relative flux density can be converted into MJy/str when multiplied by a factor 5.1×10^{-9}. This unit is astrophysical equivalent to the unit J m^{-2} (1 MJy/str = 9×10^{-20} J m^{-2})[6]. This value fluctuates in the beginning and then come closer at the maxima. Similarly in the region-1ii, relative flux density increases from 14.11 to 122.94. Initially this value is found to fluctuate and afterwards they come closer. The nature of linear plots of regions 1i and 1ii are found to be similar. Slopes of these plots are listed in Table 2. The slope of region-1ii is slightly more than that of region-1i, suggesting similar material in the region.

We study and compare the relative flux densities of the regions 2i and 2ii. In the region-2i, relative flux density goes on decreasing from eastern maxima to minima, i.e., from 122.38 to 101.00.

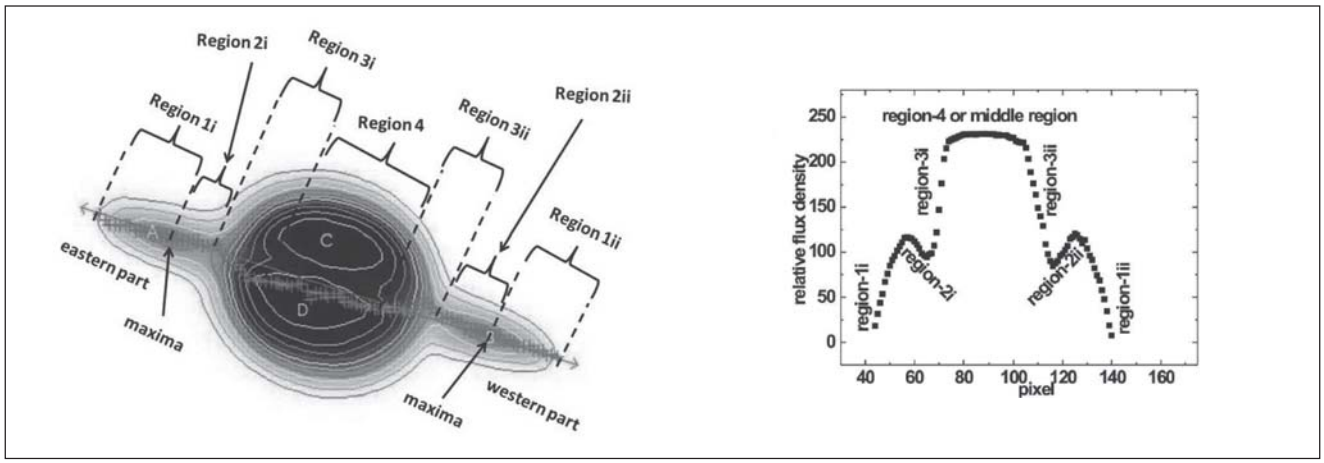

Figure 3: Image of Saturn showing contours and ticks in the image processing software ALADIN 2.5: (a) Left: The relative flux density is measured at each point (represented by the symbol '+') along the path that connects the eastern and western maxima (A & B). The region C and D represent northern and southern contours. (b) Right: The variation from eastern part to western part is classified into four regions, i.e., region-1i, 1ii, region-2i, 2ii, region-3i, 3ii and middle region or region 4.

Table 1: Values of relative flux density along line from far-western part to the far-eastern part of the ring: The first column gives the serial number for the clicks (i.e, pixels), the second and third columns give the pixel coordinates (x and y), and the last column gives the value of relative flux density (F_ν) for each pixel. It should be noted that the value of relative flux density can be converted into MJy/str when multiplied by a factor $5.1x10^{-9}$. This unit is astrophysical equivalent to the unit J m^{-2} (1 MJy/str = $9x10^{-20}$ J m^{-2})[6]. The next eight columns repeat the first four.

P	*x*	*y*	F_ν	P	*x*	*y*	F_ν	P	*x*	*y*	F_ν
1	103.18	323.00	24.55	21	124.62	329.38	102.72	41	144.37	337.50	237.55
2	104.37	324.19	38.28	22	125.62	329.56	101.00	42	145.31	337.56	237.00
3	105.25	325.12	50.17	23	126.62	329.44	104.27	43	146.37	339.00	237.22
4	106.50	325.31	60.17	24	127.68	329.31	105.27	44	148.31	339.13	237.55
5	107.56	325.50	73.39	25	128.50	330.19	113.72	45	149.25	339.50	237.61
6	108.68	325.31	82.55	26	129.50	331.37	128.66	46	150.12	339.50	237.61
7	109.56	325.55	91.50	27	130.56	332.44	153.22	47	150.81	340.19	237.22
8	110.62	326.38	97.72	28	131.68	333.56	182.72	48	152.06	339.56	237.27
9	111.62	326.31	102.11	29	132.43	334.50	209.88	49	152.87	339.50	237.27
10	112.68	326.56	107.94	30	133.56	335.50	221.61	50	153.50	340.19	236.00
11	113.75	326.62	112.83	31	134.31	336.69	229.38	51	154.25	341.12	236.55
12	114.62	327.00	117.16	32	135.50	336.19	231.11	52	155.00	341.25	236.16
13	116.00	327.56	122.50	33	136.62	336.81	232.27	53	155.81	341.19	236.16
14	117.18	327.50	122.88	34	137.75	336.94	233.44	54	156.68	341.69	236.22
15	118.31	328.25	122.38	35	138.93	336.94	234.66	55	157.68	342.13	234.38
16	119.25	328.25	121.33	36	139.93	337.13	235.94	56	158.50	342.19	233.44
17	120.56	328.50	118.44	37	140.43	337.31	237.05	57	159.43	341.94	233.27
18	121.68	328.44	114.61	38	141.31	337.63	236.94	58	160.43	342.81	229.88
19	119.68	327.94	108.12	39	142.31	337.38	237.22	59	161.18	342.63	228.38
20	123.62	328.50	105.05	40	143.25	338.00	237.05	60	162.00	342.81	228.16

Similarly in the region-2ii, relative flux density decreases from maximum to minimum value, i.e., from 122.94 to 90.67. The minimum values of flux density are found at the inner contour close to the Saturn's surface. The nature of linear plots of regions 2i and 2ii is similar (see Fig. 5). The slopes of these plots are comparable (Table 2). The slope of region-2ii is slightly more than that of region-2i. It shows that relative flux density decreases sharply than that of region-2i.

In the region-3i, relative flux density increases from minimum to maximum value, i.e., from 104.27 to 237.05 (Table 1). Similarly in the region-3ii, relative flux density is increases gradually from 96.72 to 236.22. These variations are shown in Fig. 6.

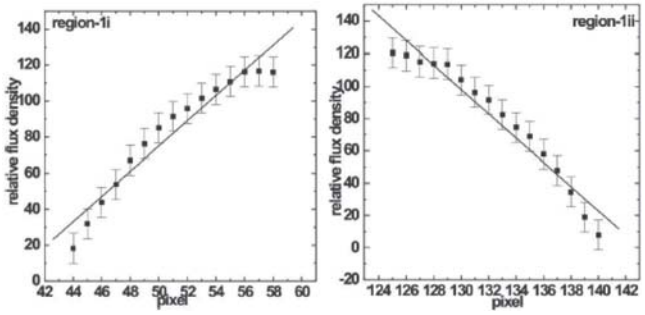

Figure 4: Region-1i & 1ii shows the relative flux density variation in the far-eastern and far-western part of the Saturn's ring. A similar feature can be seen. Solid lines represent the best fit.

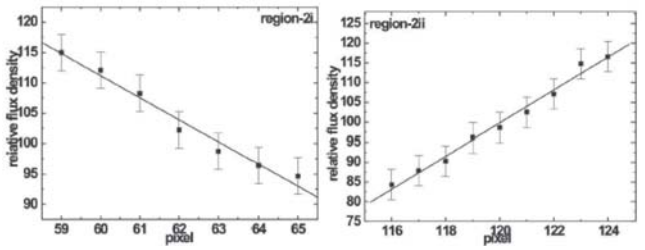

Figure 5: Region-2i & 2ii shows the relative flux density variation in the mid-eastern and mid-western part of the Saturn's ring. A similar trend can be seen. Solid lines represent the best fit.

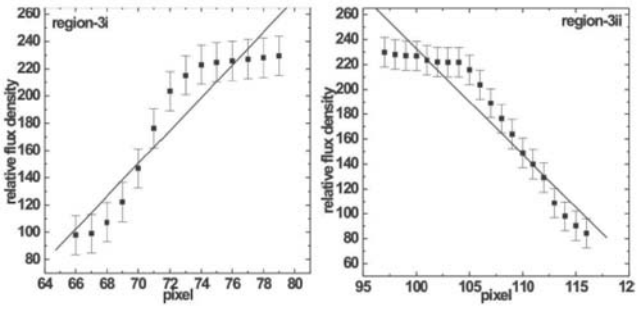

Figure 6: Region-3i & 3ii shows the relative flux density variation in the mid-eastern and mid-western part of the Saturn's ring. A similar trend can be seen. Solid lines represent the best fit.

Table 2: First column give the region. The next two columns list the values of slope (m) and intercept (c) in the best fit lines of Fig. 4-6. The last column shows the regression probability in slopes.

Region	Slope (m)	Intercept (c)	Regression Probability in slope
1i	7.008	-275.25	58.4%
1ii	-7.552	1075.93	69.3%
2i	-3.642	329.74	95.2%
2ii	4.162	399.69	98.0%
3i	12.041	-692.49	44.2%
3ii	-8.485	1081.18	60.5%

The nature of linear plots of regions 3i and 3ii is similar. The slopes of these regions are comparable (Table 2). The slope of region-3i is more than that of the slope of region-3ii. In all cases, the regression probability in the slopes are found to be more than 40% (Table 2), suggesting a good correlation between the eastern and western ring. It should be noted that the value of relative flux density can be converted into MJy/str when multiplied by a factor $5.1x10^{-9}$. This unit is astrophysical equivalent to the unit J m^{-2} (1 MJy/str = $9x10^{-20}$ J m^{-2})[6]. We can see in Table 2 that the value of relative flux density per pixel is maximum for line 1 and minimum for line 4.

CONCLUSION

A series of observation (Nov 2009 – April 2010) were carried out in order to study the flux density variation along Saturn's ring. For this, 16 inch Schimdt telescope located at Nagarkot is used. The FITS image of the planet is captured by Meade 1600 LX200GPS Schmidt-Cassegrain telescope using the software AUTOSTAR SUITE3.08 and the image is processed in the software ALADIN2.5. The values of relative flux density in 256 x 256 pixels are used for the study. We made an attempt to study the flux density variation along Saturn's ring from eastern to western region. The observed two-dimensional image of the ring is divided into five regions namely far-eastern, mid-eastern, middle, mid-western, far-western. We found that the total flux sometimes increases and sometimes decreases showing peak values at different regions along the ring. However, in the middle (across the planet), we found a fairly homogeneous emission. We took data of relative flux density in each pixel in these regions. The minimum and maximum values of flux density are found to lie in the range $(5.9 – 12.7) \times 10^{-7}$ MJy/str. The absorption feature is found to be prominent in western region.

We conclude our result as follows:

(1) As we go from eastern to western region along the path of Saturn's ring, the relative flux density increases and decreases on many occasions showing peak values at different positions.

(2) The central part of the planet showed homogeneous emission. This region showed maximum emission ~ 12-13 x 10^{-7} MJy/str.

(3) The mid-eastern and mid-western regions in Saturn's ring showed minimum emission (5.5-6.5 x 10^{-7} MJy/str), i.e., maximum absorption.

(4) The values of flux density are found to lie in the range $(5.9 – 12.7) \times 10^{-7}$ MJy/str.

The above mentioned result showed that the emission and absorption features along the planet Saturn's ring vary inconsistently. Probably the role of materials present in Saturn and its ring is important. A three dimensional study of the ring is essential to understand the absorption feature in detail.

ACKNOWLEDGEMENTS

We are highly indebted to Prof. U. Khanal for his timely suggestion. We acknowledge B.P. Koirala Memorial Planetarium, Observatory and Science Museum Development Board, Ministry of S&T, Government of Nepal for providing several observing nights for the observation and also for local accommodation facility. One of the authors (HPN) acknowledges the board for providing the scholarship for this work.

REFERENCES

[1] Hamilton, C. 1997. *Voyager Saturn Science Summary*, Solarviews.

[2] Gibilisco, S. 2003. *Astronomy Demystified*, McGraw-Hill.

[3] Karttunen, H., Kroger, P., Oja, H., Poutanen, M. and Donner, K.J. 2007. *Fundamental Astronomy Fifth Edition*. Springer-Verlag.

[4] Operating Manual 2003: *8", 10", 12", 14", 16" LX200GPS Schmidt-Cassegrain Telescopes*, Meade Instruments Corporation.

[5] Working Manual 2002: *CCD Camera Models ST-7XE, ST-8XE, ST-9XE, ST-10XE, ST-10XME and ST-2000XM*, Santa Barbara Instrument Group.

■